# Amplification of ultra-short laser pulses via resonant backward Raman amplification in plasma

S. K. Mishra[1,a)] and A. Andreev[1,2,a)]
[1]ELI-Attosecond Light Pulse Source, Szeged, Hungary
[2]MBI, Berlin, Germany

(Received 17 June 2016; accepted 18 July 2016; published online 4 August 2016)

In this paper, we have examined the possibility of using resonant backward Raman amplification (BRA) as an efficient mechanism in amplifying the low intensity ultra-short ($\leq$fs) pulses using plasma as intermediate amplifying medium; such pulses are anticipated to get produced in the form of the secondary sources at ALPS (Attosecond Light Pulse Source) center of ELI (Extreme Light Infrastructure). In preliminary assessment of the scheme, the analytical expressions for the pump/seed laser pulses and plasma characteristic features are obtained which concisely describe the parameter regime of resonant BRA applicability in achieving significant amplification. The consistency of the scheme in the context of ELI-ALPS sources has been validated through particle in cell (PIC) simulations. The peak intensity of the amplified seed pulse predicted via simulation results is found in reasonable agreement with the analytical estimates. Utilizing these analytical expressions as a basis in perspective of ELI-ALPS parameter access, a specific example displaying the key plasma and laser parameters for amplifying weak seed pulse has been configured; the limitations and conceivable remedies in resonant BRA implementation have also been highlighted. *Published by AIP Publishing.* [http://dx.doi.org/10.1063/1.4960216]

## I. INTRODUCTION

The procurement of high-intensity ultra-short radiations through amplification and compression of the short laser pulses[1–3] is one of the principal focus among the physics frontiers on account of its wide range of implications towards science and engineering aspects;[4] this includes plasma based particle acceleration,[5] inertial confinement fusion,[6] and practical realization of fundamental atomic state/quantum physics.[7] Apart from the well versed CPA (chirped pulse amplification) technique[1–3] available for the generation of short-intense pulses, backward Raman amplifiers (BRAmp) have theoretically been presented[8–13] and further have experimentally[14–23] been verified as a significant contrivance to achieve the un-focused laser intensities up to relativistic regime. The plasma in this course is specified as appropriate amplifying medium which can tolerate and mediate much larger fluence than any usual material grating. The scheme of backward Raman amplification (BRA) is based on the concept of stimulated Raman scattering where the small signal with stokes frequency along with pump gets amplified keeping all the features of input signal intact. From the application perspective, BRA scheme exploits the notion of resonant energy transfer from large energy pump pulse to short Raman down-shifted seed pulse in counter streaming geometry via electrostatic Langmuir plasma waves.[8] In this process, the seed pulse captures much higher energy from the pump effectively in shorter duration and may also lead to the compression of the seed pulse.[10] The efficiency of the resonant BRA is restricted by nonlinear effects associated with plasma perturbations invoked at relativistic laser intensities; the nonlinear processes may include amplified pulse filamentation,[8] relativistic detuning,[24,25] parasitic forward Raman scattering,[8] pulse depletion/plasma heating through inverse bremsstrahlung,[10] Langmuir wave Landau damping[26–28] or breaking,[9] and others.[29–32] Most of these venomous processes can be handled by reasonable and cautious choices of laser and plasma parameters.[33] In recent years, numerous theoretical/analytical/simulation and consequent experimental[8–28] studies have been discerned in order to overcome with these nonlinear effects and optimize the efficiency of amplified seed pulse. One of the noticeable outcomes is the experimental verification of the suppression of deleterious Raman instability of the pump to noise ratio via appropriate detuning of the three wave resonance by implementing the pump frequency chirp or plasma density gradient.[9,21] From the literature, it is fairly evident that the resonant BRAmp can be utilized an efficient tool to achieve the robust laser intensities, and in this present study, we apply this aspect in examining its significance in amplifying the low energy ultra-short (sub-femto second) pulses. Such weak ultra-short pulses are anticipated to be produced in second phase campaign at Extreme Light Infrastructure-Attosecond Light Pulse Source (ELI-ALPS) as secondary sources.[34–37]

## II. ANALYTICAL EXPRESSIONS FOR RESONANT BRA

BRA mechanism eventually refers to the light and plasma wave coupling where the seed pulse with a down-shifted frequency is nourished by significant energy transfer from a high energetic pump pulse through an excited plasma wave, by the virtue of the three wave interaction process. The resonant condition, in order to achieve significant

a)Electronic addresses: nishfeb@gmail.com and alexanderandreev72@yahoo.com

amplification, using the conservation of momentum and energy, can be written as

$$\boldsymbol{k_0} - \boldsymbol{k_1} = \boldsymbol{k_2} \quad \text{and} \quad \omega_0 = \omega_1 + \omega_2, \tag{1}$$

where $\boldsymbol{k_j}$ and $\omega_j (= 2\pi c/\lambda_j)$ refer the wave vector (in medium) and the frequency associated with interacting waves, $c$ is the speed of light, while $\lambda_j$ indicates the wavelength; the subscripts $j$, i.e., 0, 1, and 2, correspond to the pump, seed, and plasma parameters, respectively. The first identity is the vector sum of the wave numbers for counter streaming pulses ($k_0$ and $k_1$ are in the opposite directions) and plasma wave ($k_2$) during amplification, while the second identity refers the frequency match between the pump, seed, and plasma wave.

Resonant BRA is a consequence of three wave decay process where the pump loses its energy to the counter propagating seed and the plasma wave. The resonant Langmuir ($L$-) plasma wave is characterized by the dispersion relation $\omega_2^2 = \omega_p^2 + v_{th}^2 k_2^2$, where $v_{th}$ refers to thermal speed of electrons and $\omega_p$ is the plasma frequency corresponding to plasma slab with electron density $n_e$. Considering that the plasma is not too hot (i.e., $k_2 v_{th} \ll \omega_p$), this relation simply reduces to $\omega_2 \approx \omega_p = (4\pi n_e e^2/m_e)^{1/2}$, where $e$ and $m_e$ correspond to the electronic charge and mass, respectively; for analytical practice, this simplified relation is safely applicable as far as the electron temperature $T_e \leq 0.01 m_e c^2 \sim 5\,\text{keV}$. The propagation of pump and seed laser pulses in the plasma is specified by dispersion relation $\omega_{0,1}^2 = \omega_p^2 + c^2 k_{0,1}^2$; in this configuration, the critical plasma density corresponds to downshifted seed pulse and can be written as $n_{cr} = (m_e \omega_1^2/4\pi e^2)$. It is well understood from the earlier investigations that the backward Raman amplification process holds efficiently in the under critical plasma regime. We use a recent work by Malkin and Fisch[38] to obtain the expressions in order to scale and estimate the features of output signal and necessary physical properties of the BRAmp; their analysis for the amplification of short (~ps) pulses takes account of simple analytical estimates based on slowly varying envelope approximation (*svea*). Prior to proceed further in the analysis, it is customary to refine the validity of *svea* in the context of ultra-short (~fs) pulses. *Svea* in time domain states that the variation in amplitude can be considered to be small enough over a time period of oscillation; empirically, *svea* can be expressed as $\partial_t^2 A \ll \omega \partial_t A \Rightarrow \tau_l(as) \gg (1/2)\lambda(\text{nm})$, where $\tau_l$ refers the time scale of intensity variation. From analysis perspective, $\tau_l$ can be taken as $\sim \tau_o/10$, where $\tau_o$ refers *fwhm* of the pulse. Hence, the inequality should read as $\tau_o(as) \gg 5\lambda(\text{nm})$ and straightaway predicts that *svea* is well applicable for the shorter wavelengths but longer pulses. For a particular example, say, for $\lambda \approx 1\,\text{nm}$, *svea* is valid only if $\tau_o \gg 5\,\text{as}$ or reasonably pertinent for an ~20 as pulse; this statement affirms that the applicability of analytical expressions may also be extended to ultra-short (~fs-as) regime with a cautious choice of pulse features.

In the three wave interaction process, the excited Langmuir ($L$) plasma wave procures the fraction $(\omega_2/\omega_0)$ of the energy from the laser pump. If any damping loss from the $L$-wave is ignored during the energy acquisition from the pump and its transfer to the seed pulse, the sustenance of $L$-wave is limited ideally by the wave breaking phenomenon, which occurs when the electron gains quiver velocity larger than the phase velocity of the $L$-wave. Hence, the peak intensity of the pump corresponding to the $L$-wave breaking threshold can be given by $I_{br} = (n_e/n_{cr})^{3/2}(4\omega_1\omega_0/c^2k_2^2)I_M$, where $I_M \approx (n_{cr} m_e c^3/16)$. It should also be mentioned that the $L$-wave breaking is avoidable below the threshold pump power ($I_0 < I_{br}$) and thus we confine our analysis in this particular regime where the hydrodynamic/fluid description is pertinent. The pump laser in extreme ultraviolet (XUV) spectral regime may correspond to typical solid state plasma density, and in order to achieve efficient BRA, the absorption of the pump pulse energy via inverse bremsstrahlung (electron-ion collisions) during amplification should be minimized; this criteria may pose a minimal condition on the plausible length of the amplifying plasma channel and algebraically can be expressed as $l < c/\nu_{ib} \sim (\omega_0^2/\omega_2^2)(c/\nu_e)$, where $\nu_e$ is the effective collision frequency of electrons in the plasma. In linear regime of resonant BRA process where the pump pulse depletion is negligible, the largest possible linear growth rate of the seed pulse corresponding to the Stokes wave can be written as[38] $\gamma_0 \sim (\omega_1/\omega_0)[(\omega_0\omega_2/32)(I_0/I_M)]^{1/2} s^{-1}$. It can evidently be noticed from the expression of growth rate that in case $n_e \ll n_{cr}$, below wave breaking threshold $\gamma_0$ is much smaller than the plasma frequency, i.e., $\gamma_0 \ll \omega_2 \sim \omega_p$. As the pump pulse (relatively longer) encounters with the shorter and weaker backward propagating seed pulse, in the linear regime the seed pulse fed by intermediate $L$-plasma wave and its amplitude grows exponentially.[38] It infers that the amplitude maximum of the amplified seed pulse propagates with speed $\sim c/2$, while front moves with light speed $\sim c$ and hence in the linear regime the seed pulse displays broadening. In the pump depletion regime, the growth is no longer exponential but much slower and thus the number of exponentiations occurred in seed pulse during the amplification time remains roughly the same, viz., $\Lambda_0 \sim 2\gamma_0\sqrt{(t - z_M/c)t}$, where $z_M$ refers the position of seed pulse intensity maximum in amplification. In order to achieve significant amplification of the seed pulse, the value of $\Lambda_0$ should be chosen such that it could completely superimposed with $L$-wave plasma noise exponentiations ($\Lambda_p$) during amplification,[38] i.e., $\Lambda_0 < \Lambda_p$, where $\Lambda_p \sim (1/2)\ln(2\lambda_0^2 I_0 \omega_2/T_e\gamma_0^2)$ and $T_e$ is plasma temperature. The maximum amplitude achieved by the seed pulse (i.e., leading spike) in this case can be approximated as $I_1 \sim 8I_0(\gamma_0^2 t^2/\Lambda_0^2)$ with the duration $\Delta t_1 \sim (\Lambda_0/\gamma_0^2 t)$. The value of $\Lambda_0$ also yields a notion of initial seed features (intensity/width) as it ultimately leads to the pulse amplification. A relation between the initial seed intensity ($I_{1o}$), initial pulse width ($\Delta t_{1o}$) and $\Lambda_0$ can be read as[38] $I_{1o}\Delta t_{1o}^2 \approx I_M(256\pi\Lambda_0)(\omega_0/\omega_1)^2 \exp(-2\Lambda_0)/(\omega_0\omega_2)$; this expression infers that for two known parameters out of three (i.e., $I_{1o}, \Delta t_{1o}, \Lambda_0$), a plausible value of third one can be obtained. Further, if the seed is amplified up to relativistic intensities, the growth of the seed pulse eventually in the depletion region is restricted by relativistic nonlinearity created by the leading spike of

the seed pulse.[38] This causes a finite phase change ($\delta_o$) during the wave interaction and the large variation in phase may lead a change in the energy transfer rate/direction during the wave interaction (pump to seed or vice versa). Thus, the amplification time (or plasma length) should be kept short enough to avoid such a large phase change in relativistic regime, viz., below the maximum amplification time $t_M$ and can be written as $t < t_M \approx (1/\omega_2)[3\delta_o(16\Lambda_0 I_M/I_0)^2(\omega_0/\omega_1)]^{1/3}$. The maximum achievable duration of the leading spike of the seed can thus be given by

$$\Delta t_1 \sim (\Lambda_0/\gamma_0^2 t) > \Delta t_{1m} \approx (\omega_0/\omega_1)^2(4/\omega_0)[(2\Lambda_0 I_M/3\delta_o I_0)(\omega_1/\omega_0)]^{1/3}. \quad (2)$$

Corresponding fluence can be written as $w_1 \sim (I_1 \Delta t_1) < w_{1m} \approx (64 I_M/\omega_2)[(3\delta_o I_0/2\Lambda_0 I_M)(\omega_0/\omega_1)]^{1/3}$.

This refers to the largest achievable intensity as

$$I_1 < I_{1m} \approx (w_{1m}/\Delta t_{1m}) \sim (\omega_1/\omega_0)^2(16 I_M \omega_0/\omega_2)[(3\delta_o I_0/2\Lambda_0 I_M)(\omega_0/\omega_1)]^{2/3}. \quad (3)$$

The largest output pulse fluences and intensities are achieved in the plasma of lowest possible density still in the hydrodynamic limit, namely, wave-breaking density, i.e., $\omega_2 \sim \omega_1 (c^2 k_2^2 I_0/4\omega_1\omega_0 I_M)^{1/3}$. Maximizing the above expressions over the plasma density at wave breaking density, the maximum achievable intensity can be put as follows:

$$I_{max} \approx 16(I_M^2 I_0)^{1/3}(3\delta_o \omega_1/c k_2 \Lambda_0)^{2/3}. \quad (4)$$

The above expressions are applicable to the under critical plasma regime with moderate plasma density. It should also be noted here that in the strongly under critical regime of the plasma ($n_e \ll n_{cr}$), $ck_2 \approx 2\omega_0$ and the expressions for maximum fluence and the intensity reduces to the expressions as obtained in Ref. 38.

Another concern with resonant BRA is the premature Raman backscattering where the plasma noise grows slower in comparison to the pump perturbations; this might prematurely deplete the pump energy much earlier to seed encounter and inhibit significant coupling between the pump and the seed pulse. In order to avoid premature backscattering and ensure the maximum amplification of the seed pulse, detuning of the Raman resonance is an effective tool which suppresses the unwanted-nonresonant exponentiations of the linear Raman growth;[9] the detuning process is usually accomplished via a frequency chirping of the pump pulse or by creating a finite density gradient of the amplifying plasma medium. Thermal agitation of the plasma due to intense lasers may also give rise to Landau damping of the *L*-waves and certainly may inhibit the significant energy transfer to the seed pulse. To prevent the amplification from this deleterious effect, the thermal electron velocity (corresponding to plasma temperature) should be kept much smaller than that of *L*-wave phase velocity, viz., $T_e \ll (m_e c^2/4)(\omega_2^2/\omega_0^2) \equiv T_M$. The above expressions (Eqs. (2)–(4)) and the physics constraints can be utilized to configure an appropriate set of laser/plasma parameters for the experimental campaign in order to achieve significant amplification/compression of the seed pulse; a particular example, taking specific pump/seed pulse and consistent plasma parameters relevant to ELI-ALPS infrastructure, has been discussed in Sec. III.

## III. PARAMETRIC CONFIGURATION FOR RESONANT BRA REALIZATION AT ELI-ALPS FACILITY

We utilize the physical expressions obtained in Sec. II to establish a parameter regime where the efficient amplification of the low intensity ultra-short pulses anticipated at ELI-ALPS through secondary sources could be achieved. It is clear from the above discussion that the primary laser parameters at ELI-ALPS facility are not consistent to use it as pump in BRA processing for secondary sources (seed pulse); an alternative pump source could be the free electron lasers (FEL) which can efficiently be produced by using *PW* lasers. The lasers which will be installed as primary sources at ELI-ALPS facility,[34–37] can be used for efficient electron bunch acceleration ($I_0 \sim 10^{21}\,\mathrm{W/cm^2}$, i.e., $a_0 \sim 21$, $\lambda \approx 800\,\mathrm{nm}$) and refers to the energy gain by a single electron $\sim$10 MeV. The electron bunch with this energy equivalence can be used as electron source for the preliminary injection to the undulators in FEL; this is in well resemblance with the typical energy gained by electron bunch in *RF* gun operation stage ($\sim$5 MeV) used in standard FEL.[39–41] In particular, the output pulse of FEL of the Fermi light source[41] is specified by the spectral range $\sim$20–100 nm, peak power $\sim$10 GW, and the pulse length $\sim$30–100 fs over the spot size $\sim$140–290 $\mu$m which corresponds to the intensity $\sim 10^{13}\,\mathrm{W/cm^2}$. Such FEL infrastructure can be developed using the present setup available at ELI-ALPS and can be used as a pump laser source for BRAmp. In order to meet the user's requirement, the focal spot of the output photon beam needs to be optimized. The total reflective optics in Kirkpatrick–Baez (*K–B*) geometry, which combines a pair of grazing-incident mirrors in an orthogonal arrangement,[42–44] seems to be the most promising technology in achieving high efficiency with a broad spectral acceptance. A system likewise can be adopted to optimize the focal spot and intensify the pulse; thus, one can speculate that with the proper technological adjustment, the anticipated FEL pump pulse can further be compressed spatially to a $\sim\mu$m size spot and thus the intensities of the order of $\sim 10^{18}\,\mathrm{W/cm^2}$ can be achieved. A feasible schematic of BRAmp setup, consistent with ELI-ALPS parameter access, has been illustrated in Fig. 1.

The thickness of the plasma layer required as amplifying medium in the present context, which should be of the order of half of the pump pulse duration ($\sim$10s $\mu$m), raises another concern in pursuing this scheme, viz., the generation of such thin plasma layers of the order of solid density. Such thin plasma layers are presumed to be generated via illuminating the target surface through the long duration intense laser pulses;[20,45] for example, $\sim$100 $\mu$m width plasma of nearly solid density ($\sim 10^{22}\,\mathrm{cm^{-3}}$, 100 eV) has experimentally[45] been obtained. With the similar assessment, in a recent work, Sadler *et al.*[46] have argued the use of high density ($\sim 5\times 10^{22}\,\mathrm{cm^{-3}}$, 200 eV) thin CH plasma slab ($\sim$40 $\mu$m).

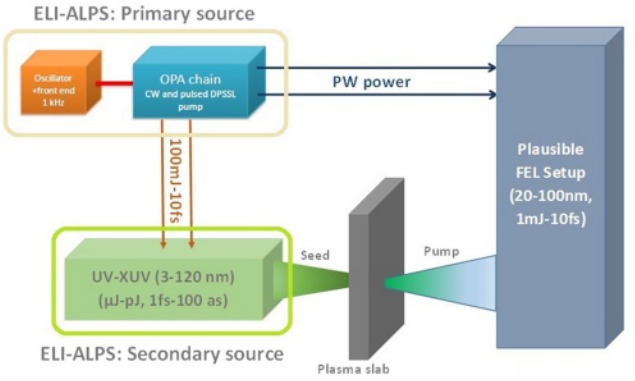


FIG. 1. A schematic of the feasible BRAmp setup, relevant to ALPS infrastructure.

Thus, with this notion, similar arrangement can be proposed to generate such plasma layers using ELI-ALPS laser; of course, the technological implementation is a challenging task as the plasma becomes inhomogeneous at the surface for such short scale lengths. As the high intensity pump pulse enters in this plasma slab, the plasma temperature may get raise and may be crucial to BRA process as it leads to pulse filamentation. The plasma temperature can be estimated by using the balance of the energy gained by plasma electrons due to laser heating and conductive loss through the slab; in the steady state, this can be expressed as $J.E \approx \nabla.(\chi_e \nabla T_e)$, where $J$ is the plasma current density, $E$ is the laser pulse electric field, and $\chi_e = (5k_b^2 n_e T_e/m_e \nu_e)$ and $\nu_e (= 3.7 n_e \ln\Lambda/T_e^{3/2})$ refer thermal conductivity and effective electron collision frequency, respectively. Assuming uniform temperature, the energy balance of electrons in the plasma can be written as $J.E \sim n_e \nu_e a_0^2 (m_e c^2) \approx (\chi_e T_e/l^2)$; thus, $T_e \approx [l(3.7 n_e \ln\Lambda)(a_0 m_e c/k_b)]^{2/5}$. This expression predicts that the plasma temperature in general increases with the increase in plasma density ($n_e$), slab width ($l$), and laser pulse intensity. In reference to this temperature, the characteristic length[47] of the thermal filamentation of the laser pulses can be written as $l_{fil}/\lambda_0 \sim 8(\omega_0^2/\omega_2^2)(v_t^2/a_0^2 c^2)$ and should be much larger than the amplifying medium in order to avoid the thermal filamentation of constituent laser pulses.

As discussed earlier, we will use quasi-FEL source to perform this particular assessment; for example, the pump may be specified with intensity $I_0 \approx 10^{17}\,\mathrm{W/cm^2}$ ($\lambda_0 \approx 40\,\mathrm{nm}$). A plausible preliminary laser parameter for the ultra-short seed pulse ($\lambda_1 \approx 60\,\mathrm{nm}$), viz., the pulse length and energy, has been taken from Refs. 34–37. In consistency with *svea*, we take $\tau_1 \sim 1\,\mathrm{fs}$ seed pulse into account to commence further parametric configuration. The specific pump and seed pulse parameters used for illustration are listed in top two panels of Table I. The plasma density, consistent with the resonant BRA condition (Eq. (1)), is found to acquire a moderate value ($n_e \leq n_{cr}/4$) because such a plasma has been revealed to be advantageous for the seed amplification/compression.[13] The pump intensity taken herein is well below the $L$-wave breaking threshold intensity ($I_0 \sim I_{br}/122$). For this case, the seed pulse may acquire the significant linear growth rate $\gamma_0 \approx 1.5 \times 10^{14}\,\mathrm{s^{-1}}$. The maximum amplification of the output seed pulse amplitude is

TABLE I. Plausible parametric configuration for resonant BRA realization at ELI-ALPS facility.

| | |
|---|---|
| Plausible pump laser parameters | |
| Wave length $\lambda_0$ | $\sim 40\,\mathrm{nm}$ |
| Pulse frequency $\omega_0$ | $\sim 4.71 \times 10^{16}\,\mathrm{s^{-1}}$ |
| Pulse length $\tau_0$ | $\sim 10\,\mathrm{fs}$ |
| Peak intensity ($I_0$) | $\sim 10^{17}\,\mathrm{W/cm^2}$ (spot size $\sim 10\,\mu\mathrm{m}^2$) |
| Plausible seed laser parameters | |
| Wave length $\lambda_1$ | $\sim 60\,\mathrm{nm}$ |
| Pulse frequency $\omega_1$ | $\sim 3.14 \times 10^{16}\,\mathrm{s^{-1}}$ |
| Pulse length $\tau_1$ | $\sim 1\,\mathrm{fs}$ |
| Pulse energy $\varepsilon_1$ | $\sim 10\,\mathrm{nJ}$ |
| Peak power $W_1$ | $\sim 10\,\mathrm{MW}$ |
| Peak intensity $I_1$ | $\sim 10^{14}\,\mathrm{W/cm^2}$ (spot size $\sim 10\,\mu\mathrm{m}^2$) |
| Output results | |
| Wave breaking Int. $I_{br}$ | $\sim 1.22 \times 10^{19}\,\mathrm{W/cm^2}$ |
| Plasma density $n_e$ | $\sim 7.82 \times 10^{22}\,\mathrm{cm^{-3}}$ |
| $L$-$w$ frequency $\omega_2$ | $\sim 1.57 \times 10^{16}\,\mathrm{s^{-1}}$ |
| Pulse duration ($\delta t_s$) | $\sim 2.2\,\mathrm{fs}$ |
| Output fluence $w_{1m}$ | $\sim 1.6 \times 10^4\,\mathrm{J/cm^2}$ |
| Output intensity $I_{1m}$ | $\sim 7.1 \times 10^{18}\,\mathrm{W/cm^2}$ |
| Amplification factor ($I_{1m}/I_1$) | $\sim 7.1 \times 10^4$ |
| Maximum amplification time ($t_M$) | $\sim 160\,\mathrm{fs}$ |
| Maximum plasma thickness ($l_p \sim ct_M$) | $\sim 48\,\mu\mathrm{m}$ |

determined by the numbers of seed pulse exponentiations $\Lambda_0$ in the amplifying plasma. For the initial seed pulse features (pulse width/intensity) consistent with parameter access ELI-ALPS facility, one gets $\Lambda_0 \approx 8$. For the pump laser and plasma parameters in the present case, one gets $T_e \sim 1.5\,\mathrm{keV}$ and corresponds to the $L$-wave noise exponentiations $\Lambda_p \sim 11$; this value of $\Lambda_p$ is slightly higher than $\Lambda_0$ and consistent with the obligation of significant overlapping of seed and $L$-wave to achieve prominent amplification. Further, in sake of the convenience, a plausible value relativistic nonlinear phase shift $\delta_o = 1$, compliant to tolerable nonlinear phase detuning of the resonance,[38] is taken for further parametric evaluation. In reference to Eq. (4), the maximum intensity achieved by the seed pulse after amplification in the resonant case is $I_{1m} \approx 10^{19}\,\mathrm{W/cm^2}$. Subsequently, the shortest achievable duration of the leading spike in the output seed pulse can be expressed by Eq. (2) as $\delta t_s \approx \Delta t_{1m} \approx 2.2\,\mathrm{fs}$. It is instructive to note here that the typical pulse width of the secondary sources at ELI-ALPS facility is anticipated to be of the order of ~(10 as–1 fs); thus, the pulse compression is little difficult in the parameter space considered herein, specifically if the pulse is in attosecond regime; of course, the significant amplification in the amplitude is noticed to acquire through resonant BRA. Nonetheless, one can anticipate operating in scenario where the pump intensity approaches to $L$-wave breaking threshold ($I_{br} \sim 1.22 \times 10^{19}\,\mathrm{W/cm^2}$), the pulse may be compressed to ~400 as. The seed pulse evaluation leads to maximum possible amplification time $t_M \approx 160\,\mathrm{fs}$, preventing the amplification from any loss due to relativistic phase detuning; this certainly limits the maximum duration of pump pulse ($\tau_0 \sim 2t_M$) and hence the plasma width ($l \leq ct_M \approx 48\mu\mathrm{m}$). The criteria for the length of the plasma should also be scaled through a

condition, viz., smallness of the laser energy absorption (inverse-bremsstrahlung[10]) and can be expressed as $l < c/\nu_{ib} \sim 700\,\mu$m; the sterner one between the two limits should be preferred for plasma scaling. Further as noticed in this case $T_e \ll T_M$, Landau damping of the $L$-waves during amplification can safely be ignored, in the present context. The characteristic filamentation length with respect to this plasma temperature estimate results in $l_{fil} \sim 300\,\mu$m and hence the thermal filamentation does not seem to inhibit the amplification process in the present framework. The maximum plausible plasma length ($l \approx 48\,\mu$m) indicates that the pump pulse retains large number of exponentiation ($\Lambda_m \sim \gamma_0 t_M \approx 24$) during amplification ($\sim t_M$) than that of seed ($\Lambda_0 \sim 8$) and $L$-wave plasma noise ($\Lambda_p \sim 11$); this certainly might lead the system to premature pump depletion. To prevent the pump pulse from parasitic backscattering due to plasma noise, the scheme of frequency chirp linear detuning of the Raman resonance can be utilized by putting the condition on the frequency detuning factor as $\Lambda_0^{-1} > (\delta\omega_{dt}/\gamma_0^2 t) > \Lambda_p^{-1}$. For this particular case, one can choose the linear instability associated with pump to make 10 exponentiations and this might lead to a time evolving $\delta\omega_{dt} = (\gamma_0^2 t/10)$; the maximum possible frequency detuning corresponds to amplification time $t_M$ as $\delta\omega_{dt} \sim 2\gamma_0 \approx 3 \times 10^{14}\,\mathrm{s}^{-1}$. This estimate detuning factor is nearly 1% of the pump frequency and can be manifested via chirping the pump laser or alternatively by implementing plasma density variation by ~6%. Following Malkin and Fisch,[38] it is also of interest to note that in the absence of the detuning, the amplification in terms of output intensity suppresses by a factor of $\sim(\Lambda_p^2/\Lambda_m^2) \approx 0.25$ only. The preliminary pump/seed laser pulse parameters used for exemplifying the conceptual basis and outcome estimates, exploring the possibility of seed pulse amplification/compression, evaluated in this section have been summarized and listed in Table I.

## IV. THE SIMULATION SCHEME AND RESULTS

In this section, the seed pulse amplification has been verified via 1D relativistic electromagnetic particle in cell (PIC) simulation code.[48] In order to simulate the resonant BRA, in simulation scheme we take account of the interaction between the counter propagating harmonics of a reference fundamental frequency ($\omega_f$), as it facilitates the analysis with first two harmonics. To mimic laser and seed wavelengths, we use $\omega_f = 1.57 \times 10^{16}\mathrm{s}^{-1}$ as a fundamental frequency in the simulation and the plasma parameters is established via the frequency matching between plasma and pump/seed frequencies; the pump and seed pulse frequencies in this configuration thus can be referred as $\omega_0 = 3\omega_f$ and $\omega_1 = 2\omega_f$. In the resonant case ($L$-wave frequency $\omega_2 = \omega_0 - \omega_1$), this should be equal to the fundamental frequency $\omega_2 = \omega_f$) and the resonant plasma density $n_c = 7.82 \times 10^{22}\,\mathrm{cm}^{-3}$. To conduct the simulation run, a $\sin^2$ temporal profile of the pulse is used. As per the simulation requirement, the pulse should be terminated when its amplitude is physically insignificant in comparison to its peak value; in this framework, the pulse is terminated at a reasonable width, i.e., $\tau_{(0,1)p} \sim 8\tau_{(0,1)fwhm}$. The simulation box has been specified in three regions where the incident-transmitted zone is mediated by the plasma medium. The dimensions (in the units of $\lambda_f \approx c/\tau_o$) of these regions are kept consistent with the pump/seed pulse parameters; the seed pulse (from left end) is considered to hit the plasma layer when the pump pulse front approximately reaches to left edge of the plasma slab. The pump and seed pulses are chosen of *fwhm* ~10 fs and 1 fs, respectively, for numerical simulation. The pump and seed pulses counter propagate through a plasma, and in this process, the seed pulse gets amplified by a large factor where the energy transfer from the pump pulse is mediated by the plasma perturbations. For the simulation, $a_0 \sim 0.1 (I_0 \sim 10^{18}\,\mathrm{W/cm^2} \approx I_{18})$ and $a_1 \sim 0.001 (I_1 \sim 10^{14}\,\mathrm{W/cm^2} \approx 0.1 I_{15})$, corresponding to pump and seed pulses, are used as the normalized laser fields. Both the resonant and non-resonant phases of Raman amplification of the seed pulse have been analyzed and discussed. The effect of varying peak pump intensity on the amplification of the seed pulse in resonant BRA regime has been displayed in Fig. 2; the snapshot of the field profile has been taken at the end of the simulation time and the two pulses (seed/pump) do not influence each other further. The peak electric field of the seed pulse is seen to amplify by a large factor (say two orders of magnitude) due to resonant BRA and thus the intensity of the input seed is enhanced by four orders of magnitude. The simulation runs for the two cases, viz., $a_0 \sim 0.05$ and 0.2, shown in Fig. 2 indicate the enhancement in the normalized field of the seed pulse, viz., 26 and 656 times, respectively; in terms of real units, these estimates refer to the output (amplified) seed pulse intensity as $\sim 6.8 \times 10^{16}\,\mathrm{W/cm^2}$ and $4.25 \times 10^{19}\,\mathrm{W/cm^2}$, respectively. In snapshots, it is noticed that the leading spike of the seed pulse after amplification is asymmetric in nature, as the leading half front is broader and the rear half portion is relatively smaller in time; it signifies that the seed front acquires larger fraction of energy than that of rear part and can be noticed in Fig. 2(b). Interestingly, this is similar to the results noticed in work by Hur *et al.*,[49] where the resonant energy exchange to the seed pulse is attributed to phase matching in the three wave interaction, in principle due to resonant conditions (Eq. (1)). Herein present analysis, this aspect has properly been imbedded in defining the initial simulation features. Further, the significant energy exchange is also evident from the departure of pump pulse from its original Gaussian profile and reduction in its intensity/energy (left half of the panel graphs in Fig. 2), after passing through the plasma. Through these results, it is noticed that the seed pulse amplification is quite sensitive to the pump intensity and it becomes more pronounced as the pump approaches to relativistic intensity. The output (transmitted) seed pulse however is seen to be distorted than its initial profile, and the leading spike of the seed pulse gets shortened with increase in the pump intensity; the Fourier transformation on the transmitted pulses has been performed and the amplified seed pulse is verified to comprise original mean frequency as a dominant component in its spectral configuration. For the same set of data used for this calculation, we have made amplification estimates on the basis of analytical expressions, and in order to make it appropriate with simulation

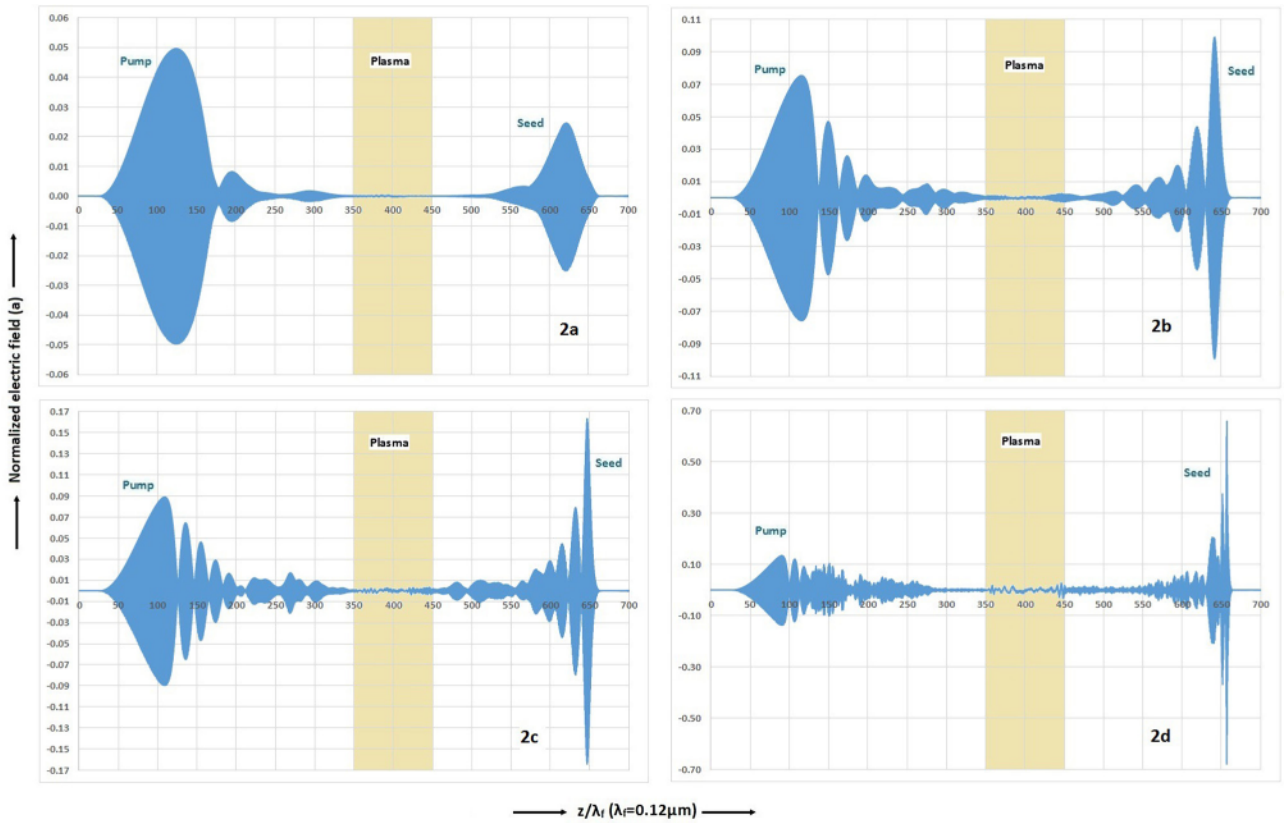


FIG. 2. Simulation results: Snapshot of the normalized electric field profile of the counter propagating pump and seed pulse at the end of the simulation (∼700 cycles); the simulation refers to pump pulse with $\lambda_0 = 40$ nm, $\tau_0 = 10$ fs ($\tau_{0p} = 80$ fs), seed pulse with $I_1 \approx 0.1I_{15}$, $\lambda_1 = 60$ nm, $\tau_1 = 1$ fs ($\tau_{1p} = 8$ fs), and the plasma density ($n_e$) corresponds to the resonant condition $\lambda_2 = 120$ nm (say $n_c$). The snapshots in the figure correspond to (a) $I_0(\sim a_0) \approx 0.25I_{18}(\sim 0.05)$, (b) $0.6I_{18}(\sim 0.08)$, (c) $I_{18}(\sim 0.1)$, and (d) $4I_{18}(\sim 0.2)$, respectively.

results, the maximum amplification is further amended by manifesting the detuning factor ($\sim\Lambda_p^2/\Lambda_m^2$). The corresponding intensity of the amplified seed pulse for both the calculations, viz., pic and analytical, has been depicted in Fig. 3. It is clearly observed that simulation results are in order of magnitude agreement with the calculations based on the analytical expressions; it is also seen that the analytical and simulation results approach reasonably close for the pump with large (viz., moderate relativistic) intensities. The consequence of the initial seed pulse intensity has also been evaluated by reducing its magnitude by a factor of 1/2 (i.e., $a_1 \sim 0.0005$) through pic calculation; as anticipated, after amplification, the seed pulse is noticed to acquire intensity equal (marginally smaller) to the case of Fig. 2. The significance of the resonant BRA operation over non-resonant

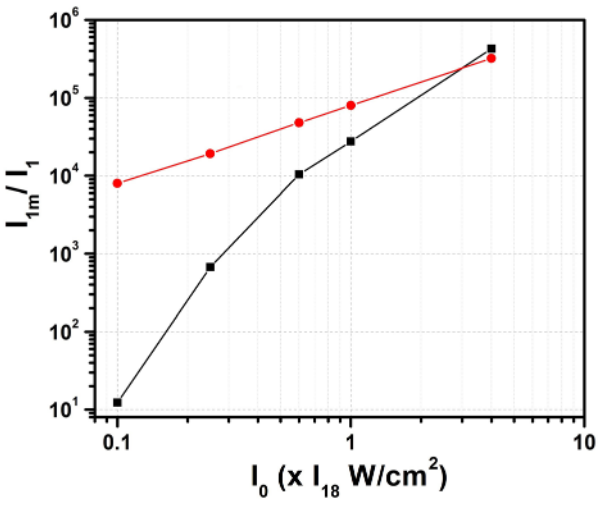


FIG. 3. The amplification factor ($I_{1m}/I_1$) of the amplified seed pulse as a function of pump intensity ($I_0$); the results refer to pump pulse $\lambda_0 = 40$ nm, $\tau_0 = 10$ fs, seed with $I_1 \approx 0.1I_{15}$, $\lambda_1 = 60$ nm, $\tau_1 = 1$ fs, and the plasma density corresponds to the resonant condition $\lambda_2 = 120$ nm ($\sim n_e \sim n_{cr}/4$). The black and red color marks refer to PIC and analytical results.

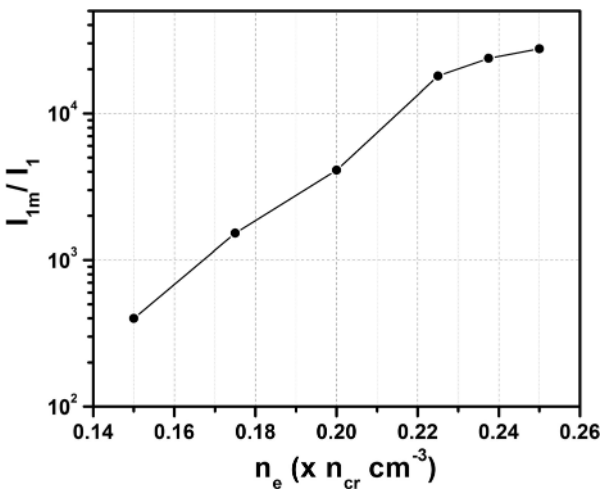


FIG. 4. The amplification factor ($I_{1m}/I_1$) of the amplified seed pulse as a function of plasma density ($n_e$); the results refer to $\lambda_0 = 40$ nm, $\tau_0 = 10$ fs, $I_0 \approx I_{18}$, $I_1 \approx 0.1I_{15}$, $\lambda_1 = 60$ nm and $\tau_1 = 1$ fs; the curves refer to PIC results.

cases has been displayed in Fig. 4 where the intermediate plasma density has been varied in order to alter the BRA system from resonant framework. The seed pulse is seen to acquire largest amplification in case of resonant case ($n_e \sim n_{cr}/4$) and the amplification continuously decreases as one moves far from resonance condition, i.e., $\omega_2 < \omega_0 - \omega_1$. The effect of input pump pulse width on the resonant amplification of the seed pulse has been displayed in Fig. 5 where the peak amplitude of the amplified seed pulse is noticed to enhance with pump pulse duration; the increase in pulse duration refers to the large energy pulse. In terms of intensity enhancement, it is raised by three times as pump duration is doubled; physically this can be understood in terms of enhanced coupling due to larger interaction time between pump and seed pulse. The consequence of initial duration of the seed pulse on its amplification for constant pump and plasma parameters has been illustrated in Fig. 6; a typical range 100 as $\leq \tau_1 \leq$ 10 fs is chosen for illustrating the effect. In this range, the amplification weakly depends on initial width of the seed pulse and is seen to optimize around $\tau_1 \sim$(1–2) fs to acquire a maximum value; this optimum pulse width is in proximity of analytical prediction of maximum achievable duration ($\Delta t_s \sim 1$ fs). For smaller seed pulses ($\tau_1 < 1$ fs), the decrease in the amplification can be attributed to the smaller energy transfer from the pump during amplification and ultimate stretching of the seed pulse ~fs duration, which results in decrease in peak intensity of the amplified seed. On the other hand, in case of large duration seed pulse ($\tau_1 \geq 2$ fs), the peak intensity decreases on account of weak overlapping between pump and seed pulse through the plasma slab ($\sim\tau_0/2$) with increasing $\tau_1$. The increase in leading spike duration eventually reduces the peak intensity, as reflected in Fig. 6; however, this drop in peak intensity is marginal (~a factor of 1/2) in comparison to enhancement factor (~4 orders of magnitude). It is also of interest to point out that the graph also specifies significant domain where *svea* is safely applicable ($\tau_1 \geq 0.5$ fs) for the

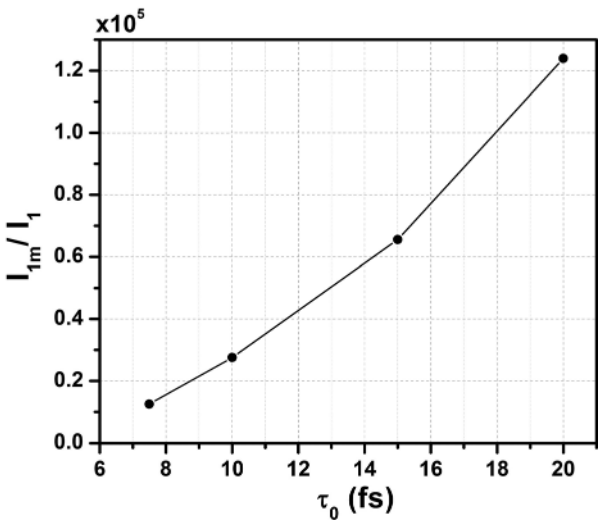


FIG. 5. The amplification factor ($I_{1m}/I_1$) of the amplified seed pulse as a function of the pump duration ($\tau_0$); the results refer to $\lambda_0 = 40$ nm, $I_0 \approx I_{18}$, $I_1 \approx 0.1I_{15}$, $\lambda_1 = 60$ nm, $\tau_1 = 1$ fs, and $n_e \sim n_{cr}/4$ (resonant case); the curves refer to PIC results.

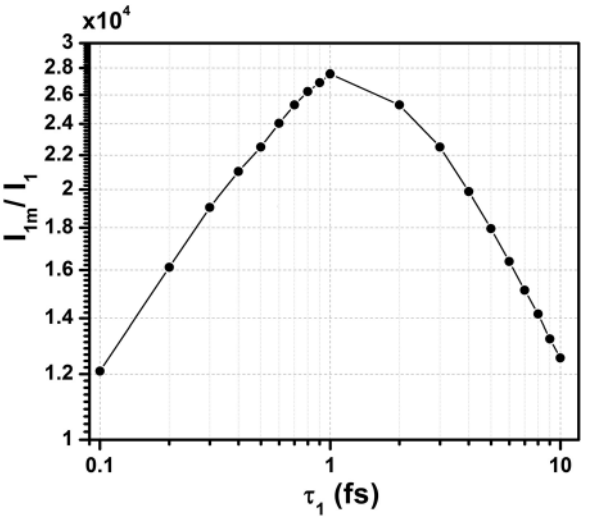


FIG. 6. The amplification factor ($I_{1m}/I_1$) of the amplified seed pulse as a function of the seed duration ($\tau_1$); the results refer to $\lambda_0 = 40$ nm, $I_0 \approx I_{18}$, $I_1 \approx 0.1I_{15}$, $\lambda_1 = 60$ nm, $\tau_0 = 10$ fs, and $n_e \sim n_{cr}/4$ (resonant case); the curves refer to PIC results.

analysis perspective. So far, the simulation results for laser/plasma parameters consistent with the parameters access at ELI-ALPS centre demonstrate that the weak seed pulse can significantly be enhanced by utilizing resonant BRAmp.

## V. SUMMARY AND CONCLUSION

In this study, we have configured a parameter regime for the laser/plasma features, using the model formulas for the practical realization of resonant BRA in the plasma for low intensity ultra-short pulses; the significance of this parametric configuration has been exemplified in the context of ELI-Alps laser facilities as a basis. In order to design the appropriate parameter regime, the analytical formulation takes precautions associated with *L*-wave breaking, premature backscattering of pump, pump absorption through inverse bremsstrahlung, Landau damping of *L*-wave, thermal filamentation of lasers, and relativistic nonlinear/thermal noise effect into account. It is instructive to note here that the formulation is quite simplified as other coexisting unwanted effects may certainly limit the seed pulse amplification in resonant BRA processing; this may include relativistic filamentation/detuning of the amplified seed pulse, parasitic effects by plasma noise on scattering of pump/amplified seed, plasma heating through inverse bremsstrahlung, 2d-transverse nonlinear effects (like pulse filamentation/self-focusing), etc. Nonetheless, the analytical formulation and expressions illustrated herein establish a notion of the parameter regime where the BRA can be performed with prominent efficacy. An estimate, taking into account the pump/seed pulse consistent with parameter access at ELI-ALPS infrastructure as an example, the key physical parameters relevant to achieve efficient resonant BRA have been listed in Table I. The proof in principle of this scheme in the context of seed pulse amplification has been verified with the simulation. The analytical and simulation results of the seed pulse amplification are found to be in a reasonable agreement; this also accomplishes the fact that the basic expressions can be

utilized in parameter designing for an experimental campaign. Our data show that for suitable choice of parameters, the seed pulse can be intensified by a large factor (∼four/five orders of magnitude), but the pulse compression is little difficult, specifically if the pulse is in attosecond regime. The numerical analysis presented herein is strained to 1D framework and does not mimic 2D transverse nonlinear effects (e.g., laser filamentation/self-focusing) which may certainly be of significance as the seed approaches to relativistic intensities. On the basis of understanding through this study, it may be concluded that the resonant BRAmp can be utilized as an efficient contrivance to amplify the ultra-short weak secondary source pulses accessible at ELI-ALPS facility and achieve high intensity short duration pulses of practical significance; of course the full fleshed operation of resonant BRA scheme at ELI-ALPS needs additional technological features to be developed.

## ACKNOWLEDGMENTS

One of the authors (S.K.M.) thank to Dr. L. Zsolt for providing the code and initial briefing.

[1]D. Strickland and G. Mourou, Opt. Commun. **56**, 219 (1985).
[2]M. Aoyama, K. Yamakawa, Y. Akahane, J. Ma, N. Inoue, H. Ueda, and H. Kiriyama, Opt. Lett. **28**, 1594 (2003).
[3]J. Faure, Y. Glinec, J. J. Santos, F. Ewald, J.-P. Rousseau, S. Kiselev, A. Pukhov, T. Hosokai, and V. Malka, Phys. Rev. Lett. **95**, 205003 (2005).
[4]E. Gerstner, "Extreme light," Nature **446**, 16–18 (2007).
[5]E. Esarey, C. B. Schroeder, and W. P. Leemans, Rev. Mod. Phys. **81**, 1229 (2009).
[6]M. Tabak, J. Hammer, M. E. Glinsky, W. L. Kruer, J. Woodworth, E. M. Campbell, M. D. Perry, and R. M. Mason, Phys. Plasmas **1**, 1626 (1994).
[7]J. Schwinger, Phys. Rev. **82**, 664 (1951).
[8]V. M. Malkin, G. Shvets, and N. J. Fisch, Phys. Rev. Lett. **82**, 4448 (1999).
[9]V. M. Malkin, G. Shvets, and N. J. Fisch, Phys. Plasmas **7**, 2232 (2000).
[10]V. M. Malkin, N. J. Fisch, and J. S. Wurtele, Phys. Rev. E **75**, 026404 (2007).
[11]V. M. Malkin and N. J. Fisch, Phys. Rev. E **80**, 046409 (2009).
[12]R. M. G. M. Trines, F. Fiuza, R. Bingham, R. A. Fonseca, L. O. Silva, R. A. Cairns, and P. A. Norreys, Nat. Phys. **7**, 87 (2011).
[13]V. M. Malkin, Z. Toroker, and N. J. Fisch, Phys. Plasmas **19**, 023109 (2012).
[14]Y. Ping, I. Geltner, N. J. Fisch, G. Shvets, and S. Suckewer, Phys. Rev. E **62**, R4532 (2000).
[15]Y. Ping, W. Cheng, S. Suckewer, D. S. Clark, and N. J. Fisch, Phys. Rev. Lett. **92**, 175007 (2004).
[16]A. A. Balakin, D. V. Kartashov, A. M. Kiselev, S. A. Skobelev, A. N. Stepanov, and G. M. Fraiman, JETP Lett. **80**, 12 (2004).
[17]W. Cheng, Y. Avitzour, Y. Ping, S. Suckewer, N. J. Fisch, M. S. Hur, and J. S. Wurtele, Phys. Rev. Lett. **94**, 045003 (2005).
[18]R. K. Kirkwood, E. Dewald, C. Niemann, N. Meezan, S. C. Wilks, D. W. Price, and O. L. Landen, Phys. Plasma **14**, 113109 (2007).
[19]C. H. Pai, M. W. Lin, L. C. Ha, S. T. Huang, Y. C. Tsou, H. H. Chu, J. Y. Lin, J. Wang, and S. Y. Chen, Phys. Rev. Lett. **101**, 065005 (2008).
[20]J. Ren, W. Cheng, S. Li, and S. Suckewer, Nat. Phys. **3**, 732 (2007).
[21]N. A. Yampolsky, N. J. Fisch, V. M. Malkin, E. J. Valeo, R. Lindberg, J. Wurtele, J. Ren, S. Li, A. Morozov, and S. Suckewer, Phys. Plasma **15**, 113104 (2008).
[22]Y. Ping, R. K. Kirkwood, T.-L. Wang, D. S. Clark, S. C. Wilks, N. Meezan, R. L. Berger, J. Wurtele, N. J. Fisch, V. M. Malkin, E. J. Valeo, S. F. Martins, and C. Joshi, Phys. Plasma **16**, 123113 (2009).
[23]G. Vieux, A. Lyachev, X. Yang, B. Ersfeld, J. P. Farmer, E. Brunetti, R. C. Issac, G. Raj, G. H. Welsh, S. M. Wiggins, and D. A. Jaroszynski, New J. Phys. **13**, 063042 (2011).
[24]V. M. Malkin, Z. Toroker, and N. J. Fisch, Phys. Plasmas **21**, 093112 (2014).
[25]V. M. Malkin, Z. Toroker, and N. J. Fisch, Phys. Rev. E **90**, 063110 (2014).
[26]V. M. Malkin and N. J. Fisch, Phys. Plasmas **17**, 073109 (2010).
[27]M. S. Hur, R. R. Lindberg, A. E. Charman, J. S. Wurtele, and H. Suk, Phys. Rev. Lett. **95**, 115003 (2005).
[28]S. Depierreux, V. Yahia, C. Goyon, G. Loisel, P.-E. Masson-Laborde, N. Borisenko, A. Orekhov, O. Rosmej, T. Rienecker, and C. Labaune, Nat. Commun. **5**, 4158 (2014).
[29]D. S. Clark and N. J. Fisch, Phys. Plasmas **9**, 2772 (2002).
[30]N. A. Yampolsky, V. M. Malkin, and N. J. Fisch, Phys. Rev. E **69**, 036401 (2004).
[31]Z. Toroker, V. M. Malkin, A. A. Balakin, G. M. Fraiman, and N. J. Fisch, Phys. Plasmas **19**, 083110 (2012).
[32]Z. Toroker, V. M. Malkin, and N. J. Fisch, Phys. Rev. Lett. **109**, 085003 (2012).
[33]Z. Toroker, V. M. Malkin, and N. J. Fisch, Phys. Plasmas **21**, 113110 (2014).
[34]P. Dombi, J. Fulop, K. Osvay, and K. Varju, in Feasibility Study for the Scientific Case of ELI Attosecond Light Pulse Source, Hungary, 2010.
[35]G. A. Mourou, G. Korn, W. Sandner, and J. L. Collier, *ELI White Book: Science and Technology with Ultra-Intense Lasers* (Andreas Thos: Berlin, 2011).
[36]K. Awazu, P. Baum, J. Biegert, M. Bussmann, L. Cederbaum, J. P. Chambaret, D. Charalambidis, J. Collier, A. Czitrovszky, Z. Divéki, G. Djotyan, P. Dombi, M. Drescher, R. Ernstorfer, G. Faigel, I. Földes, J. A. Fülöp, E. Goulielmakis, J. Hajdu, J. Hebling, K. Hideghéty, J. Honrubia, M. Kalashnikov, S. Karsch, U. Kleineberg, M. Kling, F. Krausz, G. Korn, P. Lambropoulos, R. Levine, V. Malka, R. López-Martens, F. Martin, M. Marklund, J. Meyer-terVehn, G. Mourou, D. Neely, M. Nisoli, Z. Oláh, K. Osvay, G. Paulus, F. Pfeiffer, L. Paulette, F. Quere, F. Remacle, A. Rudenko, G. Sansone, E. Springate, M. Stockman, G. Szabó, S. Szatmári, T. Tajima, H. Takabe, F. Tavella, J. Tisch, M. Tolley, C. Tóth, G. Tsakiris, P. Tzallas, K. Varjú, S. Varró, L. Veisz, M. Vrakking, T. Wittmann, and M. Wolf, in *Planned Research Activities, ALPS-ELI*, Hungary, 2012, p. 239.
[37]See http://www.eli-hu.hu/ for ELI-ALPS.
[38]V. M. Malkin and N. J. Fisch, Eur. Phys. J. **223**, 1157 (2014).
[39]W. A. Barletta, J. Bisognano, J. N. Corlett, P. Emma, Z. Huang, K.-J. Kim, R. Lindberg, J. B. Murphy, G. R. Neil, D. C. Nguyen, C. Pellegrini, R. A. Rimmer, F. Sannibale, G. Stupakov, R. P. Walker, and A. A. Zholent, Nucl. Instrum. Methods Phys. Res., Sect. A **618**, 69 (2010).
[40]See http://flash.desy.de/accelerator/ for FLASH-FEL source parameters.
[41]See https://www.elettra.trieste.it/lightsources/elettra/machine.html for FERMI-FEL source parameters.
[42]L. Raimondi, C. Svetina, N. Mahne, D. Cocco, A. Abrami, M. De Marco, C. Fava, S. Gerusina, R. Gobessi, F. Capotondi, E. Pedersoli, M. Kiskinova, G. De Ninno, P. Zeitoun, G. Dovillaire, G. Lambert, W. Boutu, H. Merdji, A. I. Gonzalez, D. Gauthier, and M. Zangrand, Nucl. Instrum. Methods Phys. Res., Sect. A **710**, 131 (2013).
[43]H. Yumoto, H. Mimura, T. Koyama, S. Matsuyama, K. Tono, T. Togashi, Y. Inubushi, T. Sato, T. Tanaka, T. Kimura, H. Yokoyama, J. Kim, Y. Sano, Y. Hachisu, M. Yabashi, H. Ohashi, H. Ohmori, T. Ishikawa, and K. Yamauchi, Nat. Photonics **7**, 43 (2013).
[44]C. Svetina, C. Grazioli, N. Mahne, L. Raimondi, C. Fava, M. Zangrando, S. Gerusina, M. Alagia, L. Avaldi, G. Cautero, M. de Simone, M. Devetta, M. Di Fraia, M. Drabbels, V. Feyer, P. Finetti, R. Katzy, A. Kivimäki, V. Lyamayev, T. Mazza, A. Moise, T. Möller, P. O'Keeffe, Y. Ovcharenko, P. Piseri, O. Plekan, K. C. Prince, R. Sergo, F. Stienkemeier, S. Stranges, M. Coreno, and C. Callegari, J. Synchrotron Radiat. **22**, 538 (2015).
[45]L. B. da Silva, R. C. Couble, and S. B. Libby, in *E&TR*, 1995, pp. 9–19.
[46]J. D. Sadler, R. Nathvani, P. Oleśkiewicz, L. A. Ceurvorst, N. Ratan, M. F. Kasim, R. M. G. M. Trines, R. Bingham, and P. A. Norreys, Sci. Rep. **5**, 16755 (2015).
[47]R. Bingham, R. Short, E. Williams, D. Villeneuve, and M. Richardson, Plasma Phys. Controlled Fusion **26**, 1077 (1984).
[48]R. Lichters, R. E. W. Pfund, and J. Meyer-ter-Vehn, *LPIC++*, Report No. MPQ 225, Max-Planck-Institute of Quantum Optics, Garching, Germany (1997).
[49]M. S. Hur, J. Kim, D. N. Gupta, H. J. Jang, and H. Suk, Appl. Phys. Lett. **91**, 101501 (2007).